Coherence Expectation Minimisation and Combining Weighted Multitaper Estimates

1st Oskar Keding
Centre for Mathematical Sciences
Lund University
Lund, Sweden
oskar.keding@matstat.lu.se

2nd Maria Åkesson
Centre for Mathematical Sciences
Lund University
Lund, Sweden
maria.akesson@matstat.lu.se

3rd Maria Sandsten
Centre for Mathematical Sciences
Lund University
Lund, Sweden
maria.sandsten@matstat.lu.se

***Abstract*—Coherence is a useful measure in many engineering applications. Here, we focus on the case where the input signal to a linear system can be measured free from noise, but the output signal is perturbed by noise. A novel expression for the expectation of a multitaper magnitude squared coherence estimate for this case is presented and verified through numerical evaluation. Additionally, the expression is used to optimise a multitaper coherence estimation method, which gives improved coherence estimation in detection. A clever combination of two weighted magnitude squared coherence multitaper estimators yields a new method, called Combined Weighted Multitaper Coherence (CWMC). The method is evaluated and compared to the Thomson multitaper method for simulated data and on real visual evoked potential electroencephalogram data, showing consistent improvement using CWMC.**

***Index Terms*—coherence, magnitude squared coherence, multitaper, spectral analysis, signal detection**

I. Introduction

To identify a linear single-input single-output system, a useful measure to inspect is the magnitude squared coherence (MSC) between the input and output signals. MSC shows the frequencies where spectral components are present and phase-locked in a pair of signals. This has been proven useful in multiple areas of system identification and is contemporarily used in engineering and science applications ranging from mechanical engineering [1] to neuroscience applications [2]–[4].

The coherence has been studied for many years with the statistics given in [5]–[8] where the Welch method is the commonly applied spectral estimator, [9]. Thomson has proposed the use of multitapers, [10], [11], which have been shown to outperform the Welch method in many applications. The multitaper method is specifically applied for robust coherence estimation in adaptive estimation and in various noise environments [12]–[16].

Although the Thomson method utilises the Slepian set of windows, they are not necessarily optimal specifically for coherence estimation. Broadening the options for tapers, one option is the Peak Matched Multiple Windows (PMMW) [17], which are designed for peak shaped spectra. A model spectrum is used and the multitapers are estimated as the eigenvectors from the corresponding model covariance matrix.

Thanks to the ELLIIT strategic research programme for funding.

A specific case of linear systems where an application of MSC is useful is the case where the input signals are clean measurements, and only the output signals are disturbed by noise. We denote this class of linear systems as *clean input noisy output* (CINO) systems. Many applications with clean steering input signals fit into this class, and we especially mention neural auditory tracking where the noise level of outputs is high. Noisy electroencephalography (EEG) signals showing electric potentials in the brain of a listener are to some extent correlated to the speech features of the attended speech, and this correlation is what is of interest to track. If attended speech signals are known then coherence measure can show to what extent and at which frequencies the EEG signals are linearly correlated to the speech. This can then be used to track the attention of the listener in a multi-speaker scenario [4], [18].

Primarily in this paper, an expression for the expected value of a multitaper MSC estimate using a set of windows is presented, for the case when the input signal is clean. The expression is subsequently evaluated numerically to ensure validity. Opening the possibility to statistically detect and estimate coherence, the expression can be useful for MSC method design in many application areas.

One application of the resulting MSC expectation expression is combating the problem of unevenly weighted multitaper spectral estimates. This causes mock-component peaks in spectral regions where there is signal in one of the channels but not the other and thus should ideally not show any coherence. The average of two weighted coherence estimates is used to reduce the effects of this problem and also reduce the overall standard deviation. This consequently increases the ability of the MSC to detect a correlated signal in the noise in the output channel.

In section II, the paper starts with a presentation of relevant theory and the derivation of the expectation expression of multitaper MSC estimation for a CINO system, which is then evaluated numerically. Secondly, in section III, the given application of the expression is presented, where a coherence estimator using the average of two weighted multitaper MSC estimates is developed. Simulations along with a real data application example are given in section IV and V respectively. Our work is concluded in section VI.

II. Coherence and Expectation Expression

A signal vector of length N, input signal $\boldsymbol{x}$ and output $\boldsymbol{y} \in \mathbf{R}^N$, can be viewed in the light of a linear system, of which the MSC identifies the spectral signature of the transform function. An estimate of the MSC is made as

$$\hat{C}_{xy}(f) = \frac{\|\hat{S}_{xy}(f)\|^2}{\hat{S}_{xx}(f)\hat{S}_{yy}(f)} \tag{1}$$

where $\hat{S}_{xy}(f)$ is the cross-spectral estimate calculated by

$$\hat{S}_{xy}(f) = \sum_{k=1}^{K} \alpha_k X_k(f) Y_k(f)^H \tag{2}$$

with analogue expressions for the auto-spectra $\hat{S}_{xx}(f)$ and $\hat{S}_{yy}(f)$. Subscript H denotes complex conjugate transpose. The α_k-weighted sum entails the product of discrete Fourier transforms (DFT) using K number of data windows (also called tapers). The windowed DFT at spectral frequency f is defined as

$$X_k(f) = \sum_{n=0}^{N-1} x(n) h_k(n) e^{-i2\pi f n} \tag{3}$$

$$Y_k(f) = \sum_{n=0}^{N-1} y(n) h_k(n) e^{-i2\pi f n} \tag{4}$$

or equivalently as

$$X_k(f) = \boldsymbol{h}_k \boldsymbol{\phi}(f) \boldsymbol{x}^T$$
$$Y_k(f) = \boldsymbol{h}_k \boldsymbol{\phi}(f) \boldsymbol{y}^T$$

for a chosen window vector $\boldsymbol{h}_k$ to taper the data, where $\boldsymbol{\phi} = \text{diag}[1\ e^{-i2\pi f}\ \dots\ e^{-i2\pi(N-1)f}]$ is the Fourier transform matrix. Often, the set of chosen tapers are the Slepian windows and equal weights, used in the Thomson method for spectral estimation [10]. Another set of windows, developed for mean squared error optimal estimation of spectral peaks, is the Peak Matched Multiple Windows (PMMW) [17]. These taper have declining weights associated with them, which can be seen in Figure 2.

A. Expectation of MSC

The true expected value of the coherence of a linear system,

$$E\left[\hat{C}_{xy}(f)\right] = E\left[\frac{|\hat{S}_{xy}(f)|^2}{\hat{S}_{xx}(f)\hat{S}_{yy}(f)}\right], \tag{5}$$

with input $\boldsymbol{x}$ and output $\boldsymbol{y}$, will not be possible to calculate giving some very cumbersome expressions. However, using a zeroth order Taylor expansion an approximation is found as

$$E\left[\hat{C}_{xy}(f)\right] \approx \frac{E\left[\hat{S}_{xy}\hat{S}_{xy}^H\right]}{E\left[\hat{S}_{xx}\hat{S}_{yy}\right]}, \tag{6}$$

where the (f) has been dropped for compactness. The numerator and denominator is evaluated as

$$E\left[\hat{S}_{xy}\hat{S}_{xy}^H\right] = E\left[\left(\sum_{k=1}^{K}\alpha_k X_k Y_k^H\right)\left(\sum_{l=1}^{K}\alpha_l X_l Y_l^H\right)^H\right] =$$

$$\sum_{k=1}^{K}\sum_{l=1}^{K}\alpha_k\alpha_l E\left[\left(X_k Y_k^H\right) X_l^H Y_l\right] = \sum_{k=1}^{K}\sum_{l=1}^{K}\alpha_k\alpha_l\,\Delta_n, \tag{7}$$

and

$$E\left[S_{xx}S_{yy}\right] = \sum_{k=1}^{K}\sum_{l=1}^{K}\alpha_k\alpha_l E\left[X_k X_k^H Y_l Y_l^H\right] = \sum_{k=1}^{K}\sum_{l=1}^{K}\alpha_k\alpha_l\,\Delta_d \tag{8}$$

respectively. We define a CINO system with a known input signal $\boldsymbol{x} = \boldsymbol{s}$ and output $\boldsymbol{y} = \boldsymbol{s} + \boldsymbol{e}$, for some noise $\boldsymbol{e}$. The output $\boldsymbol{y}$ could also be a linear filtering of $\boldsymbol{s}$, but this is excluded here. Denoting tapered DFT of noise as N_k, we can expand Δ_n and Δ_d to

$$\Delta_n = E[X_k X_k^H X_l X_l^H + X_k X_k^H N_l X_l^H +$$
$$X_k N_k^H X_l X_l^H + X_k N_k^H N_l X_l^H] = E[a+b+c+d]$$
$$\Delta_d = E[X_k X_k^H X_l X_l^H + X_k X_k^H X_l N_l^H +$$
$$X_k X_k^H N_l X_l^H + X_k X_k^H N_l N_l^H] = E[a+e+b+g]$$

Isserlis theorem is used, stating $E[ABCD] = E[AB]E[CD] + E[AC]E[BD] + E[AD]E[BC]$ [19]. The expectation $E[a]$ found as the first term in Δ_n as well as Δ_d is calculated as,

$$\begin{aligned} E[a] =& E\left[X_k X_k^H\right] E\left[X_l X_l^H\right] \\ &+ E\left[X_k X_l\right] E\left[X_k^H X_l^H\right] + E\left[X_k X_l^H\right] E\left[X_k^H X_l\right] \\ =&\ \ \boldsymbol{h}_k^H \boldsymbol{\phi}^H E[\boldsymbol{x}\boldsymbol{x}^H]\boldsymbol{\phi}\boldsymbol{h}_k \boldsymbol{h}_l^H \boldsymbol{\phi}^H E[\boldsymbol{x}\boldsymbol{x}^H]\boldsymbol{\phi}\boldsymbol{h}_l \\ &+ \boldsymbol{h}_k^H \boldsymbol{\phi}^H E[\boldsymbol{x}\boldsymbol{x}^H]\boldsymbol{\phi}\boldsymbol{h}_l \boldsymbol{h}_k^H \boldsymbol{\phi}^H E[\boldsymbol{x}\boldsymbol{x}^H]\boldsymbol{\phi}\boldsymbol{h}_l \\ &+ E[\boldsymbol{h}_k^H \boldsymbol{\phi}^H \boldsymbol{x} \boldsymbol{h}_l^H \boldsymbol{\phi}_H \boldsymbol{x}] E[\boldsymbol{h}_k^H \boldsymbol{\phi}^H \boldsymbol{x} \boldsymbol{h}_l^H \boldsymbol{\phi}_H \boldsymbol{x}]^H \end{aligned}$$

The expectation of the last term is zero except close to $f = 0$ and $\frac{1}{2}$ [11]. Applying the same calculations, along with the fact that $E[xy^H] = 0$, gives an expression for each term in the double sums in the MSC ratio. We find $E[b]$, $E[c]$ and $E[e]$ to be close to zero. The expectation of coherence becomes

$$E\left[\hat{C}_{xy}\right] \approx \frac{\sum_k^K \sum_l^K \alpha_k\alpha_l\,(E[a]+E[d])}{\sum_k^K \sum_l^K \alpha_k\alpha_l\,(E[a]+E[g])} = \frac{\boldsymbol{\alpha}^H \boldsymbol{U} \boldsymbol{\alpha}}{\boldsymbol{\alpha}^H \boldsymbol{L} \boldsymbol{\alpha}} \tag{9}$$

where $\boldsymbol{\alpha}$ is the vector of taper weights, while $\boldsymbol{U}$ and $\boldsymbol{L}$ are conjugate symmetric matrices in $\mathbb{C}^{K,K}$ with elements

$$\begin{aligned} U_{k,l} = T_{k,l}^1 + T_{k,l}^2 + T_{k,l}^N = \\ \boldsymbol{h}_k^H \boldsymbol{\phi}^H \boldsymbol{R_x} \boldsymbol{\phi}\boldsymbol{h}_k \boldsymbol{h}_l^H \boldsymbol{\phi}^H \boldsymbol{R_x} \boldsymbol{\phi}\boldsymbol{h}_l + \\ \boldsymbol{h}_k^H \boldsymbol{\phi}^H \boldsymbol{R_x} \boldsymbol{\phi}\boldsymbol{h}_l \boldsymbol{h}_k^H \boldsymbol{\phi}^H \boldsymbol{R_x} \boldsymbol{\phi}\boldsymbol{h}_l + \\ \boldsymbol{h}_k^H \boldsymbol{\phi}^H \boldsymbol{R_x} \boldsymbol{\phi}\boldsymbol{h}_l \boldsymbol{h}_k^H \boldsymbol{\phi}^H \boldsymbol{R_n} \boldsymbol{\phi}\boldsymbol{h}_l \end{aligned} \tag{10}$$

$$\begin{aligned} L_{k,l} = T_{k,l}^1 + T_{k,l}^2 + T_{k,l}^D = \\ \boldsymbol{h}_k^H \boldsymbol{\phi}^H \boldsymbol{R_x} \boldsymbol{\phi}\boldsymbol{h}_k \boldsymbol{h}_l^H \boldsymbol{\phi}^H \boldsymbol{R_x} \boldsymbol{\phi}\boldsymbol{h}_l + \\ \boldsymbol{h}_k^H \boldsymbol{\phi}^H \boldsymbol{R_x} \boldsymbol{\phi}\boldsymbol{h}_l \boldsymbol{h}_k^H \boldsymbol{\phi}^H \boldsymbol{R_x} \boldsymbol{\phi}\boldsymbol{h}_l + \\ \boldsymbol{h}_k^H \boldsymbol{\phi}^H \boldsymbol{R_x} \boldsymbol{\phi}\boldsymbol{h}_k \boldsymbol{h}_l^H \boldsymbol{\phi}^H \boldsymbol{R_n} \boldsymbol{\phi}\boldsymbol{h}_l \end{aligned} \tag{11}$$

where $\boldsymbol{R_x}$ and $\boldsymbol{R_n}$ are the Toeplitz covariance matrices for the signal and noise processes.

For the CINO system, as the signal-to-noise level becomes decreasingly small, the first two terms of the sums in Eqs. (10) and (11) become zero and a lowest possible expectation of the coherence measure is obtained for any combination of signals with certain noise characteristics. With evenly weighted subspectra and white noise assumption the lowest expectation is easily identified in the expression as $1/K$.

B. Evaluation of Expectation Expression

To validate the expression derived in Eq. (9) a simulation is made, where the derived expectation expression is compared to the average of $M = 10000$ multitaper estimates using the same even weights and tapers, ($K = 10$). A known AR2 process of length $N = 512$ with a peak in $\frac{1}{4}$, damping factor 0.9 and unit innovation variance, is simulated as channel $\boldsymbol{x}$ and with added white noise as channel $\boldsymbol{y}$. Simulations are repeated for added noise variances $\frac{1}{2}$, 2 and 10.

The results of the analytic calculations from Eq. (9) compared to the average of simulations are presented in Figure 1. One can see that the analytic expression follows the simulated coherence well for all three noise levels. The deviations are due to the order-zero Taylor expansion.

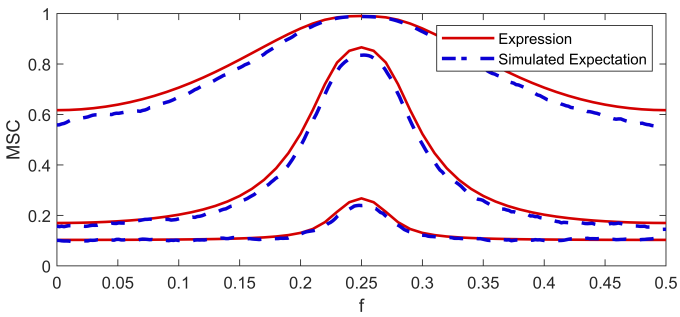

Fig. 1. The expectation of evenly weighted multitaper MSC estimation of an AR2 process as input signal, comparing the analytic expression of Eq. (9) to the average multitaper MSC estimates for simulations of the AR2 process in $\boldsymbol{x}$ and the same process with added white noise disturbance in $\boldsymbol{y}$ for the CINO model. Although deviations due to approximations are observable, the expression holds well.

III. Application of Expectation Expression To Improving Coherence Estimation

As an application where the expression derived in Eq. (9) proves useful, the expression can be reexamined as an objective function to optimise over weights $\boldsymbol{\alpha}$ in order to choose how to weigh the tapered spectral estimates in the MSC estimator.

A. Minimising Expectation Towards True Coherence

In a CINO system, the true MSC, given the true spectra of input and output processes, can be put as

$$\frac{|S_{xy}|^2}{S_{xx}S_{yy}} = \frac{|S_{xx}+S_{xe}|^2}{S_{xx}^2+S_{xx}S_{ee}} = \frac{S_{xx}^2}{S_{xx}^2+S_{xx}S_{ee}} \qquad (12)$$

To create an estimate close to the true value in Eq. (12), we aim to minimise the last two terms of the three terms in the numerator $\boldsymbol{U}$ divided by $\boldsymbol{L}$,

$$\min_{\alpha} \frac{\boldsymbol{\alpha}^H(\boldsymbol{T^2}+\boldsymbol{T^N})\boldsymbol{\alpha}}{\boldsymbol{\alpha}^H\boldsymbol{L}\boldsymbol{\alpha}}, \qquad (13)$$

where $\boldsymbol{T^2}, \boldsymbol{T^N}$ are matrices with elements given in Eq. 10. Although ideally the middle term of the three elements of $\boldsymbol{L}$ should be zero as well, this goal suffices. Especially when noise is significant, since elements of $\boldsymbol{T^2}$ will be small in comparison to the other two terms.

We constrain the minimisation to only positive weights, by asserting $\mathbf{1}^T\boldsymbol{\alpha} \geq \mathbf{0}$, to ensure stability of final coherence estimates. Minimisation on this form is done by attaching the constraint $\boldsymbol{\alpha}^H\boldsymbol{L}\boldsymbol{\alpha} = 1$ to the reduced problem

$$\min_{\alpha} \boldsymbol{\alpha}^H(\boldsymbol{T^2}+\boldsymbol{T^N})\boldsymbol{\alpha}. \qquad (14)$$

A numerical solution can be found using numerous optimisation solvers to obtain a set of weights for coherence estimation that minimises the expected coherence value in centre of the modelled spectral components.

As an example, utilising fmincon() in Matlab, an optimisation of Eq. (14) is done, in the centre frequency of a signal consisting of the peaked spectra

$$S_x(f) = \begin{cases} e^{\frac{-2C|f|}{10Blog_{10}(e)}} & |f| \leq B/2 \\ 0 & |f| > B/2 \end{cases} \qquad (15)$$

matching the PMMW use. Parameters were $C = 20$, $K = 8$ $N = 512$ and $B = (K+1)/N$, and the applied matching multitapers of the PMMW method are computed according to [17]. The additive white noise has standard deviation $\sigma_e = 0.4$ in channel $\boldsymbol{y}$. The resulting weights are shown in Figure 2 together with the given associated weights of the PMMW method.

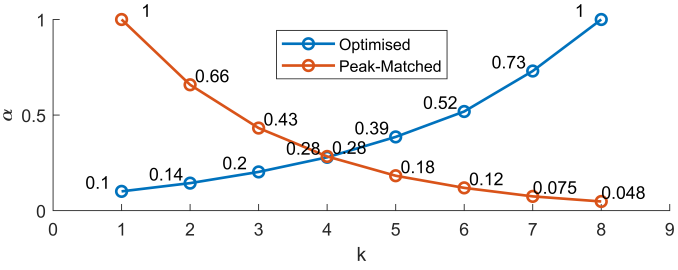

Fig. 2. The set of taper weights for coherence estimation, through optimisation described in section III-A (blue), and the PMMW associated weights (red) as calculated in [17].

B. Improving Performance of Coherence Estimation

Detecting the coherent case (C case), $\boldsymbol{y} = \boldsymbol{x} + \boldsymbol{e}$, compared to the non-coherent (NC case), $\boldsymbol{y} = \boldsymbol{e}$, is as previously stated an interesting and important problem. The detection problem constitutes multiple aspects, firstly identifying the spectral band of the correlated or non-correlated component in question. Secondly, statistically inferring the existence of the

phase-locked signal must be made by differing the y-signal samples from the NC case. Separating these cases depends on the overlap of the distributions of coherence estimates $\widehat{C}_{xy}(f)$ in both cases. We want to distinguish the two distributions from each other by separating expectations and minimising standard deviation in coherent and non-coherent cases.

To improve detection ability of correlated y-signals the estimates of two weighted multitaper coherence methods are averaged, $\widehat{C}^{D}_{xy}(f) = \left(\widehat{C}^{w_1}_{xy}(f) + \widehat{C}^{w_2}_{xy}(f)\right)/2$. Suitable choices of weights cause less correlated coherence estimates which yields two main improvements. Firstly, matching the weights to the optimised and flipped optimised weights in Figure 2 will significantly reduce the unwanted spectral peaks that exist in the weighted coherence estimates of non-coherent signal cases, which can be seen in Figure 3 for the individual coherence estimates. Additionally and perhaps more important in an application, the averaging of two estimates reduces variance of the final coherence estimate and improves detection ability of a coherence estimation algorithm. The proposed combination of coherence estimates is called Combined Weighted Multitaper Coherence (CWMC). As the same tapers are used in each coherence estimate, no DFTs have to be calculated twice, only the weighted sums and division operations.

IV. Simulations

A simulation of a linear system, for both the C case and NC case, is made to evaluate the CWMC method developed in the previous section. A clean signal $\boldsymbol{x}$ is simulated by filtering unitary-powered white noise of length $N = 128$ with peaked spectrum process (centre frequency $f_0 = 0.125$) filter by the spectra as defined in Eq. (15). The output signal is then defined as in section III-B, with additive simulated white noise ($\sigma_e = 0.4$), for both the C case and the NC case. The noise level is set so coherence detection is not trivial, but also not so difficult that difference between methods are not shown. Coherence estimates using Thomson method equal-weighted, using PMMW with the two different sets of weights derived in Section III-B, as well as the CWMC are calculated. By repeating simulations 10000 times numerical estimates of expectation as well as variation coefficient (defined as standard deviation divided by expected value) are made at each frequency for all four methods. These are shown in Figure 3. The C case is shown to the right and NC case is to the left.

In the same simulations, we extract the empirical distribution of the average of estimated coherence in the frequency band $[f_0-0.03, f_0+0.03]$, using the Thomson method and the CWMC. The distributions in the C and NC cases are shown in the left top and bottom part of Figure 4 for the CWMC and and Thomson method respectively. A receiver operating characteristic (ROC) curve is estimated from these distribution as well, shown in Figure 4. One can see that the CWMC has a consistent improvement to the detection of coherence for this signal model. Future work could entail finding better combinations of weights specifically for certain tasks such as detection.

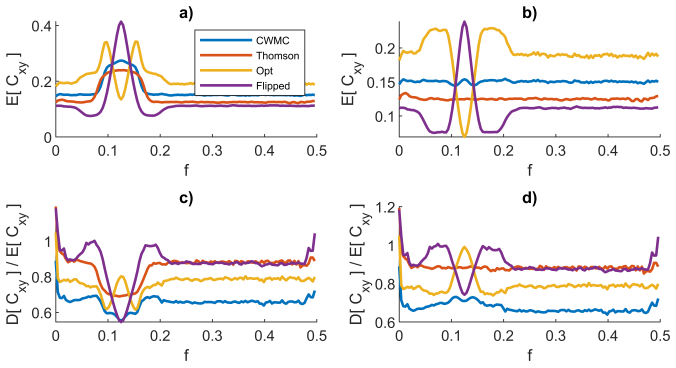

Fig. 3. A simulation of a peaked spectrum process illustrating the problem of weighted multitaper coherence estimates. Expectation and variation coefficient of coherence estimates of the Thomson method, the PMMW with two different sets of weights (Optimised and Flipped) and the CWMC method.

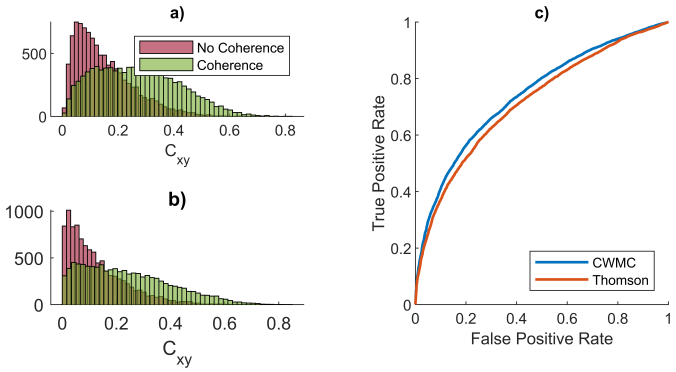

Fig. 4. A comparison of the performance of CWMC method and Thomson method for classification of the C and NC case of a peaked spectrum process in the input signal. Histogram of methods in both cases are shown for the methods; a) the CWMC method and; b) the Thomson method. In c), the resulting ROC curves for both methods are shown.

V. Real Data

We illustrate the benefits of the CWMC method with a classification example of EEG data with and without flickering light visual stimulation. Data was recorded with a final sample frequency of $F_s = 256$ Hz for a total duration of 15 seconds using a Neuroscan system with a digital amplifier (SYNAMP 5080, Neuro Scan, Inc.). Amplifier band-pass settings were 0.3 and 50 Hz. The subject had their eyes closed and was presented with flickering light for a duration of 5 seconds, 5 seconds into the recording. Four trials were made, all with different frequencies of the flickering light; 12, 15, 17 and 20 Hz. In all trials data was collected from 19 EEG channels.

Each original recording was further divided into eleven segments with 50% overlap such that all segments had a duration of 2.5 seconds ($N = 640$ samples). Six of these contained data recorded without visual stimulation, which we from heron will call class 0. Three segments contained data recorded during visual stimulation, which we denote belonging to class 1. The other two segments contained data that was recorded both with and without flashing light and were discarded. This gave a total of 456 samples belonging to

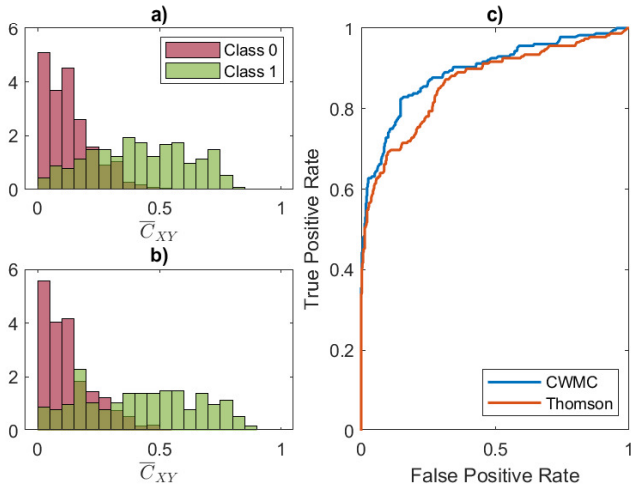

Fig. 5. Classification example of EEG signals with and without visual stimulation, denoted class 1 and 0 respectively. The normalised histograms of the average coherence $\overline{C}_{XY}$ around the correct frequency are illustrated using; a) the CWMC method and; b) the Thomson method. In c), the resulting ROC curves for both methods are shown.

class 0 and 228 samples belonging to class 1.

Furthermore, we assume that the system input signal x during visual stimulation is given by a pure sine wave with the same frequency as the presented flickering light. The CWMC and Thomson coherence spectra were calculated for each sample with a sine wave of correct frequency. As before, $K = 8$ tapers were used in the calculations. In the CWMC method, the same weights as in the simulation were used. The parameters for both methods were chosen such that the spectral bandwidth became $B = F_s(K+1)/N = 3.6$ Hz.

Finally, the average coherence within ± 1.3 Hz of the true frequency was calculated for each sample. The width was chosen to be slightly smaller than the average width of the CWMC coherence peak in class 1. The sample distributions for each class using the CWMC and Thomson coherence are shown in Figure 5(a) and (b) respectively. We note that the Thomson coherence in (b) is able to make lower estimates for class 0, and higher estimates for class 1. However, it is clearly seen that the variance of the CWMC coherence is lower for class 1 in comparison to the Thomson coherence. This makes the two classes more easy to separate using the CWMC coherence, resulting in slightly better classification performance. In Figure 5(c) the ROC, calculated using the empirical distribution of data, for the two methods are plotted and the CWMC is shown to outperform the Thomson multitaper coherence.

VI. Conclusion

We have presented an expectation expression for multitaper coherence for any signal, along with an application where the expression proves useful, in minimising the expression for choosing taper weights in a coherence estimate. Additionally, a novel coherence estimator is presented, which averages estimates from two weighted multitaper coherence estimates, one being the optimised weights and the other the flipped weight vector. The new coherence estimator outperforms coherence estimation with even weighted subspectras using Thomsons method. Improvement is shown, both in simulated peaked-spectrum signal data as well as in a real data example, detecting visually evoked potential frequencies in electroencephalography data. The derived expectation expression and the proposed novel Combined Weighted Multitaper Coherence method show possible paths for future improvement of coherence estimation of noisy signals with limited data lengths.

References

[1] D. Wang, X. Zhao, L.-L. Kou, Y. Qin, Y. Zhao, and K.-L. Tsui, "A simple and fast guideline for generating enhanced/squared envelope spectra from spectral coherence for bearing fault diagnosis," *Mechanical Systems and Signal Processing*, vol. 122, pp. 754–768, May 2019.

[2] C. S. Musaeus, K. Engedal, P. Høgh, V. Jelic, M. Mørup, M. Naik, A.-R. Oeksengaard, J. Snaedal, L.-O. Wahlund, G. Waldemar, and B. B. Andersen, "Oscillatory connectivity as a diagnostic marker of dementia due to Alzheimer's disease," *Clinical Neurophysiology*, vol. 130, no. 10, pp. 1889–1899, Oct. 2019.

[3] J. L. Meyers and et al., "A genome-wide association study of interhemispheric theta EEG coherence: implications for neural connectivity and alcohol use behavior," *Molecular Psychiatry*, vol. 26, no. 9.

[4] V. Viswanathan, H. M. Bharadwaj, and B. G. Shinn-Cunningham, "Electroencephalographic Signatures of the Neural Representation of Speech during Selective Attention," *eneuro*, vol. 6, no. 5, pp. ENEURO.0057–19.2019, Sep. 2019.

[5] S. Y. Wang, "Exact confidence interval for magnitude-squared coherence estimates," *IEEE Signal Processing Letters*, vol. 11, no. 3, pp. 326–329, March 2004.

[6] G. C. Carter, "Coherence and time delay estimation," *Proc. of the IEEE*, vol. 75, no. 2, pp. 236–255, Feb 1987.

[7] G. C. Carter and A. H. Nuttall, "Statistics of the estimate of coherence," *Proc. of the IEEE*, vol. 60, no. 4, pp. 465–466, April 1972.

[8] G. D. Brushe and J. R. Waller, "On the computation of an averaged coherence function," *Digital Signal Processing*, vol. 11, no. 2, pp. 111–119, 2001.

[9] P. D. Welch, "The use of fast Fourier transform for the estimation of power spectra: A method based on time averaging over short, modified periodograms," *IEEE Trans. on Audio Electroacoustics*, vol. AU-15, no. 2, pp. 70–73, June 1967.

[10] D. J. Thomson, "Spectrum estimation and harmonic analysis," *Proc. of the IEEE*, vol. 70, no. 9, pp. 1055–1096, Sept 1982.

[11] A. T. Walden, "A unified view of multitaper multivariate spectral estimation," *Biometrika*, vol. 87, no. 4, pp. 767–788, 2000.

[12] Y.-M. Zhang, Z. Huang, and Y. Xia, "An adaptive multi-taper spectral estimation for stationary processes." *Mechanical Systems and Signal Processing*, p. 109629, 2023.

[13] H. Zifeng and X. You-Lin, "A multi-taper S-transform method for spectral estimation of stationary processes." *IEEE Transactions on Signal Processing*, vol. 69, pp. 1452 – 1467, 2021.

[14] J. Young, V. Dragoi, and B. Aazhang, "Precise measurement of correlations between frequency coupling and visual task performance." *Scientific reports*, vol. 10, no. 1, p. 17372, 2020.

[15] J. Brynolfsson and M. Hansson-Sandsten, "Multitaper estimation of the coherence spectrum in low SNR," in *Proceedings of the EUSIPCO*, Lisbon, Portugal, 2014.

[16] M. Hansson-Sandsten, "Cross-spectrum and coherence function estimation using time-delayed Thomson multitapers," in *Proceedings of the ICASSP*. Prague, Czech Republic: IEEE, 2011.

[17] M. Hansson and G. Salomonsson, "A multiple window method for estimation of peaked spectra," *IEEE Trans. on Signal Processing*, vol. 45, no. 3, pp. 778–781, March 1997.

[18] N. Ding and J. Z. Simon, "Emergence of neural encoding of auditory objects while listening to competing speakers," *Proceedings of the National Academy of Sciences*, vol. 109, no. 29, pp. 11 854–11 859, Jul. 2012.

[19] L. Isserlis, "On a formula for the product-moment coefficient of any order of a normal frequency distribution in any number of variables," *Biometrika*, vol. 12, no. 1-2, pp. 134–139, Nov. 1918.